Influence of Metal Content on Size, Dispersion, and Magnetic Properties of Iron−Cobalt Alloy Nanoparticles Embedded in Silica Matrix

Guido Ennas,*,‡ Andrea Falqui,‡ Sergio Marras,‡ Claudio Sangregorio,† and Giaime Marongiu‡

Dipartimento di Scienze Chimiche, Università di Cagliari, S.S.554 bivio per Sestu, 09042 Monserrato (Cagliari), Italy, Dipartimento di Chimica, Università di Firenze, Via della Lastruccia 3, 50019 Sesto Fiorentino (Firenze), Italy

Received July 29, 2004. Revised Manuscript Received September 29, 2004

$(Fe_xCo_{1-x})_y(SiO_2)_{1-y}$ nanocomposites were prepared by a sol−gel method, using tetraethoxysilane and metal acetates as precursors. Two sets of xerogel samples were prepared: in the first set x was kept equal to 0.5 and four y values were selected in the range 0.02−0.2; in the second set y was kept equal to 0.1 and three samples with x equal to 0.45, 0.50, and 0.70 were prepared. The samples were characterized by X-ray diffraction, TEM, and HREM to verify the formation of the FeCo alloy nanocrystals and to investigate their structure, morphology, and composition. All samples contain spherical FeCo alloy nanoparticles uniformly dispersed in the silica matrix with average size increasing with metal content. Magnetic measurements carried out on selected samples show a superparamagnetic behavior, with blocking temperature which depends on metal load, as a consequence of particle distance variation.

Introduction

The synthesis and characterization of nanomaterials is a very exciting emerging research field which has received important scientific and technological attention.[1] Nanomaterials can be found as separate nanoparticles or as condensed bulk materials that are made of grains with size in the nanometer range. The large surface-to-volume ratio of nanoparticles greatly enhances the role played by surface atoms; as a consequence, the nanomaterial's properties (e.g., catalytic, optical, electrical, optoelectronic, mechanical, thermodynamic, and magnetic) can be largely different from those of the corresponding conventional materials. Moreover, these properties depend not only on the characteristics of individual nanoparticles, but also on their coupling and interaction. The magnetic properties are probably those which show the most dramatic dependence on particle size and on their arrangement. It is well-known that ferromagnetic materials are constituted by domains which are groups of spins all pointing in the same direction, separated by domains walls. As the particle size decreases toward a critical value, the formation of domains walls becomes energetically unfavorable, the particles consist of single magnetic domain, and superparamagnetism occurs.[2]

The interparticle interactions can be tuned by the uniform dispersion of the particles in an organic/inorganic medium (matrix), which avoids direct contact and coalescence, and can be modulated via the control of particle size and/or volume ratio between the dispersed and matrix phases. Transition from insulating to conducting regime or from isolated to cooperative magnetic behavior can be obtained.

Nanocomposites consisting of a single metal embedded in a insulating matrix (SiO_2, Al_2O_3) have been widely investigated. To our knowledge less attention has been paid to the preparation and characterization of alloy nanoparticles dispersed in a matrix, probably due to the difficulties encountered in their stabilization.

Recently our attention has been devoted to FeCo−SiO_2 nanocomposites.[3−5] These materials are of interest because FeCo alloys have attractive size-dependent magnetic properties.[6]

The synthesis and characterization of $(Fe_xCo_{1-x})_y(SiO_2)_{1-y}$ nanocomposites is reported herewith. It has been carried out with the aim of investigating the effect of both x and y values on nanoparticle dimensions, morphology, structure, and magnetic properties.

* To whom correspondence should be addressed. Fax: +39 070 6754388. Phone: +39 070 6754364. E-mail: ennas@unica.it.
‡ Università di Cagliari.
† Università di Firenze.

(1) (a) Singh Nalwa, H., Ed. *Handbook of Nanostructurd Materials and Nanotechnology*; Academic Press: San Diego, CA, 2000. (b) Klabunde, K. J.; *Nanoscale Materials in Chemistry*; Wiley-Interscience: New York, 2001. (c) Siegel, R. W. In *Fundamental Properties of Nanostructured Materials*; Fiorani, D., Sberveglieri, G., Eds.; World Scientific: London, 1994; p 3.

(2) Dormann, J. L. In *Magnetic Properties of Fine Particles*; Dorman, J. L., Fiorani, D., Eds.; North-Holland: Amsterdam, 1992.

(3) Ennas, G.; Casula, M. F.; Falqui, A.; Gatteschi, D.; Marongiu, G.; Piccaluga, G.; Sangregorio, C.; Pinna, G. *J. Non-Cryst. Solids* **2001**, *293−295*, 1.

(4) Ennas, G.; Marongiu, G.; Marras, S.; Piccaluga, G. *J. Nanoparticles Res.* **2004**, *6*, 99.

(5) Corrias, A.; Casula, M. F.; Ennas, G.; Marras, S.; Navarra, G.; Mountjoy, G. *J. Phys. Chem. B* **2003**, *107*, 3030.

(6) MacLaren, J. M.; Schulthness, T. C.; Butler, B. H.; Sutton, R.; McHenry, M. *J. Appl. Phys.* **1999**, *85*, 4833.

10.1021/cm048761e CCC: $27.50
Published on Web 12/04/2004

Table 1. Nominal Composition, Pertinent Abbreviation, and Sol−Gel Reactants Molar Ratios of the Prepared Samples

sample composition	sample abbreviation	TEOS/EtOH/H_2O molar ratio
$(Fe_{0.50}Co_{0.50})_{0.02}(SiO_2)_{0.98}$	S0250	1/55/44
$(Fe_{0.50}Co_{0.50})_{0.05}(SiO_2)_{0.95}$	S0550	1/47/81
$(Fe_{0.50}Co_{0.50})_{0.1}(SiO_2)_{0.9}$	S1050	1/47/86
$(Fe_{0.55}Co_{0.45})_{0.1}(SiO_2)_{0.9}$	S1055	1/47/86
$(Fe_{0.70}Co_{0.30})_{0.1}(SiO_2)_{0.9}$	S1070	1/47/86
$(Fe_{0.50}Co_{0.50})_{0.2}(SiO_2)_{0.8}$	S2050	1/106/210

Experimental Section

Samples were prepared by a sol−gel technique mixing ethanolic tetraethoxysilane (TEOS, Aldrich 98%; ethanol, EtOH, Carlo Erba 96%) solutions with hydro alcoholic solutions of $Co(CH_3COO)_2{\cdot}4H_2O$ (Aldrich 98%), and $Fe(CH_3COO)_2$ (Aldrich 95%). The hydrolysis−condensation reactions were promoted by adding bidistillate water and acetic acid (Aldrich 99.8%). The pH was kept in the range 3.5−4. Metal solution concentrations were selected to obtain $(Fe_xCo_{1-x})_y(SiO_2)_{1-y}$ samples with the following characteristics: (a) a fixed Fe/Co ratio ($x = 0.5$) and a selected overall metal content ($y = 0.02$, 0.05, 0.1, 0.2), hereafter S0250, S0550, S1050, and S2050, respectively (the first two numerical digits refer to overall metal content (y) and the next two refer to Fe content (x)); (b) a fixed overall metal content ($y = 0.10$) and selected Fe/Co ratios ($x = 0.5$, 0.55, 0.70), hereafter S1050, S1055, and S1070, respectively.

The molar ratios of TEOS/EtOH/water for each sample are reported in Table 1.

In a typical preparation the starting mixture was stirred for 1 h to obtain a clear sol, which was then poured into a flat Teflon beaker and allowed to gel in air at room temperature (RT). Fresh alcogel was powdered and calcined in air at 623 K for 1 h to eliminate residual water and organics. Xerogel cooled to RT was then put in a quartz reactor, heated with a ramp rate of 10 K/min, and treated at 1073 K for 2 h under a hydrogen flux. After cooling at RT, the H_2 flux was replaced by a slow commercial argon flux (impure by some ppm of oxygen) to passivate the particle surface and to prevent their ignition.

Powder X-ray diffraction (XRD) was carried out using a θ-2θ Siemens D500 diffractometer with Mo Kα radiation, equipped with a graphite monochromator on the diffracted beam. XRD data were collected by 0.04° steps in the range $8° < 2\theta < 80°$. Selected peaks were scanned with step size of 0.02° collecting at least 5000 counts for each step. Rietveld refinement was carried out using the Rietquan program[7] calculating the amorphous SiO_2 contribution to the spectra using the Le Bail model.[8] To separate the contribution due to the average crystallite size $\langle D \rangle$ (the size of coherently diffracting domains) from that due to lattice disorder, Warren−Averbach peak profile analysis was performed on selected samples using a pattern decomposition method and assuming a pseudo-Voigt function.[9] The analysis was performed on the 110/220 reflections pair of the body-centered cubic (bcc) Fe−Co alloys. The instrumental profile parameters were derived from the fitting of XRD data of standard samples. Usual recommended fitting procedures were adopted.[10]

Measurements of static magnetic susceptibilities were performed on a Cryogenics S600 Squid magnetometer equipped with a superconducting magnet producing fields up to 6.5 T. ZFC curves were obtained by cooling the samples in zero magnetic field, then applying an external magnetic field of 50 Oe, and measuring the magnetization at increasing temperatures. FC curves were then measured in the same temperature range, cooling the sample in the presence of the same external magnetic field. Qualitative evaluation of blocking temperature was performed in the range 300−1100 K on a homemade magnetic balance. Since the alloy content is not precisely known all the reported magnetic measurements refer to the entire mass of the samples to make a direct comparison of their magnetic behavior.

Transmission electron microscopy (TEM) and high-resolution electron microscopy (HREM) observations were carried using a CM30 Philips microscope equipped with a LaB_6 electron gun. The powders were dispersed in octane in an ultrasonic bath and dropped onto a lacy film of amorphous carbon mounted on a copper grid. To obtain an accurate estimation of the average particle size at least 300 particles for each sample were counted. The resulting histogram was fitted by a log-normal distribution function $P(D) = 1/(\sqrt{(2\pi)}D\sigma) \exp -[1/(2\sigma^2)(\ln D/D_0)^2]$, where σ is the standard deviation and D_0 is the mean diameter.

Results and Discussion

TEM bright field images of samples with $x = 0.5$ and y in the range 0.02−0.2 are reported in Figure 1 a−d with the pertinent size distribution function and log-normal fit. A uniform dispersion of nanoparticles in the silica matrix is present in all samples. Nanoparticles have a spherical shape as clearly evident in the HREM image in Figure 2, which shows a defect-free monocrystal whose interplanar distance value can be ascribed to bcc FeCo alloy.[11] Mean particle size (Table 2) increases with metal content from a value of 6.9 nm in S0250 to 12.3 nm in S1050. Sample S2050, the one with the highest metal content, shows a bimodal size distribution with two maxima around 11.4 and 22.6 nm, respectively.

XRD spectra of $(Fe_xCo_{1-x})_y(SiO_2)_{1-y}$ nanocomposites are reported in Figure 3 together with the Rietveld whole fitting profile. Peaks belonging to nanocrystalline phases are superimposed on the amorphous silica halos. Peak intensities of the nanocrystalline phases increase with metal content, while their broadening decreases as a consequence of the larger particle size. The prominent peaks in all the spectra are due to bcc FeCo alloy phase; some minor peaks due to β and ϵ cobalt are detectable in some samples.[5,11,12] Rietveld analysis was carried out using the following as independent parameters: (i) the amounts of crystalline FeCo alloy, β and ϵ cobalt, and of amorphous silica; (ii) the cell dimensions of crystalline phases, and (iii) the average crystallite size. The best fit values are reported in Table 3. In all samples the sum of the metallic phases amounts is lower than the nominal composition.[13] This result can be ascribed to the presence of a thin metal oxide layer on the particle surface which does not contribute to X-ray diffraction (see later), and to the presence of a fraction of the metal dispersed in the matrix at atomic level. Refinement results confirm a significant presence of β cobalt, while ϵ phase contributes only to the samples with the highest metal load. The values of the refined alloy cell parameter are in the range 0.2855−0.2865 nm, as reported for bulk alloy in the composition range

(7) Lutterotti, L.; Ceccato, R.; Dal Maschio, R.; Pagani, E. *Mater. Sci. Forum* **1998**, *278*, 93.
(8) Le Bail, A. *J. Non-Cryst. Solids* **1995**, *183*, 39.
(9) Warren, B. E. *X-ray Diffraction*; Addison-Wesley Publishing Company: Reading, MA, 1969.
(10) Young R. A. *The Rietveld Method*; IUCR Monographs; Oxford University Press: New York, 1995.
(11) PDF-2 File. JCPDS International Center for Diffraction Data, 1601 Park Lane, Swarthmore, PA.
(12) Sun, S.; Murray, C.B. *J. Appl. Phys.* **1999**, *85*, 4325.
(13) Weight percentage (wt %) and molar fraction values are very close because of the proximity of Fe_xCo_{1-x} (55.85−58.93) and SiO_2 (60.09) formula weights.

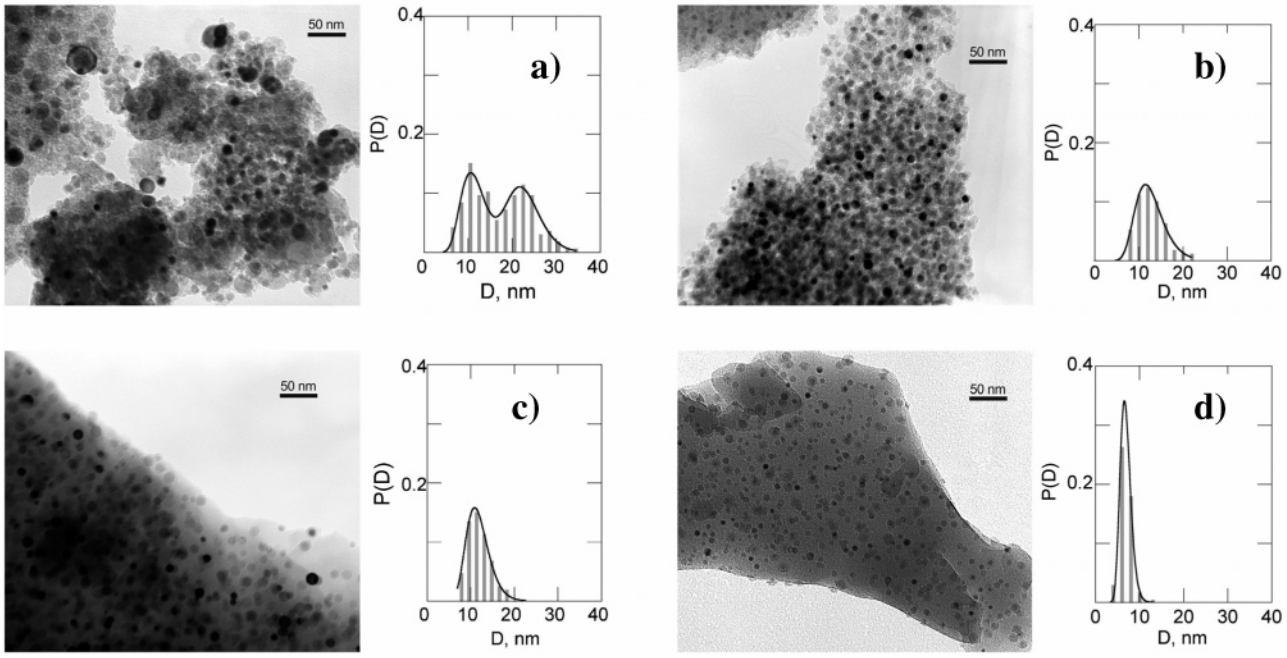

Figure 1. TEM bright field images and corresponding size histograms of (a) S2050, (b) S1050, (c) S0550, and (d) S0250 samples.

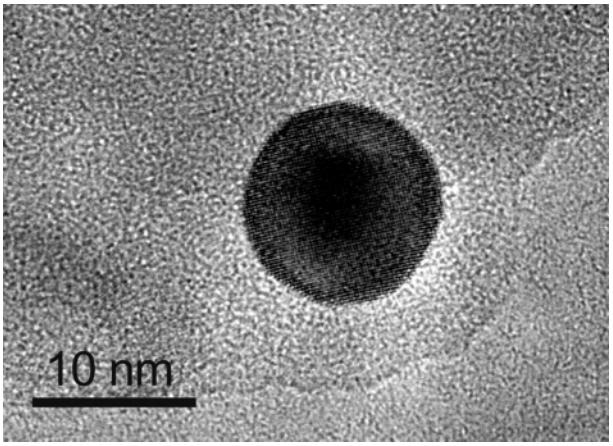

Figure 2. HREM image of S1070 sample.

Table 2. Results of Log Normal Fit of Experimental Size Distribution from TEM Images Analysis

sample name	mean particle size D_0 (nm)	relative width σ
S0250	6.9(2)	0.18(1)
S0550	11.2(2)	0.23(2)
S1050	12.3(2)	0.26(2)
S2050[a]	11.4(5)[a]	0.27(6)
	22.6(9)[a]	0.17(3)

[a] Bimodal distribution.

$Fe_{50}Co_{50}$ to $Fe_{70}Co_{30}$.[11] The values of the refined cell parameter of β and ϵ cobalt are close to those reported in the literature.[11,12] The average values of particle size increase with metal load and are in agreement with those determined by statistical analysis carried out on TEM images, if we take into account that only particle core contribute to X-ray diffraction. In the samples with $y = 0.10$ average particle size does not change with x. Rietveld analysis of S2050 sample carried out by assuming a monomodal particle size distribution gave unreasonable results. By introducing a bimodal size distribution, refinement converged to average size values comparable with those obtained by TEM, confirming the reliability of the Rietveld method. Warren Averbach peak profile analysis data lead to average particle size comparable with Rietveld analysis and indicate the absence of lattice strain.

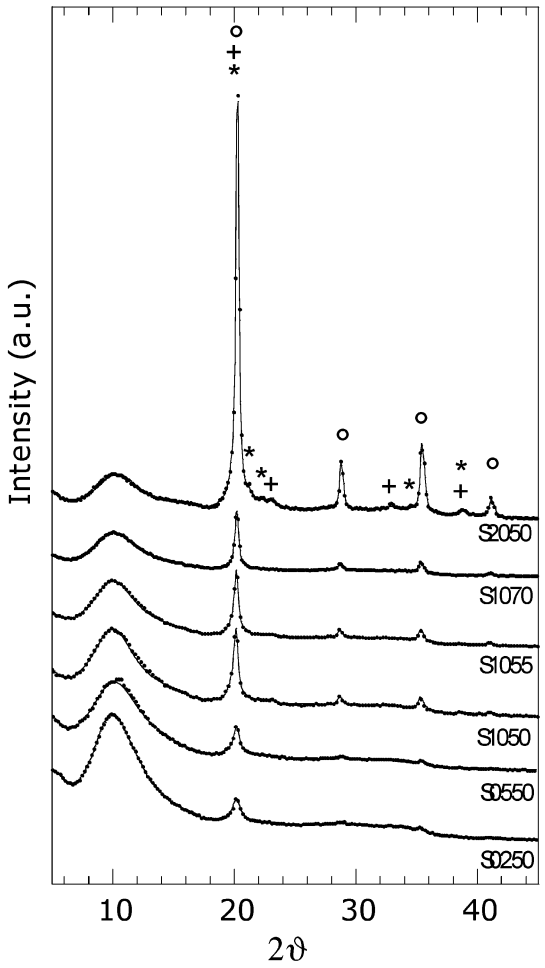

Figure 3. Experimental XRD spectra (dot) and Rietveld simulation (continuous line) of $FeCo-SiO_2$ nanocomposites: (o) FeCo, (+) β-Co, (*) ϵ-Co.

Table 3. Results of the Rietveld Refinements of XRD Data[a]

	α-FeCo			*β*-Co		*ϵ*-Co		
sample	wt %	a_0	⟨*D*⟩	wt %	⟨*D*⟩	wt %	⟨*D*⟩	R_{wp}
S0250	1.0(5)	0.2865(1)	4(1)	0.2(1)	2(1)			0.046
S0550	2.0(5)	0.2864(1)	6(1)	1.2(5)	2(1)			0.069
S1050	5.1(5)	0.2859(1)	9(1)	1.0(5)	5(1)	0.9(4)	3(1)	0.059
S1055	6.2(5)	0.2862(1)	9(1)	0.8(4)	3(1)	0.9(4)	3(1)	0.044
S1070	6.3(5)	0.2863(1)	9(1)			0.5(3)	4(1)	0.059
S2050	3.9(5)	0.2855(1)	8(1)	1.7(5)	5(1)	2.8(5)	3(1)	0.069
	10.9(5)	0.2860(1)	24(2)					

[a] Weight percentage (wt %), lattice parameters a_0 (nm), average particle size ⟨*D*⟩ (nm), and weighted pattern agreement index R_{wp}.

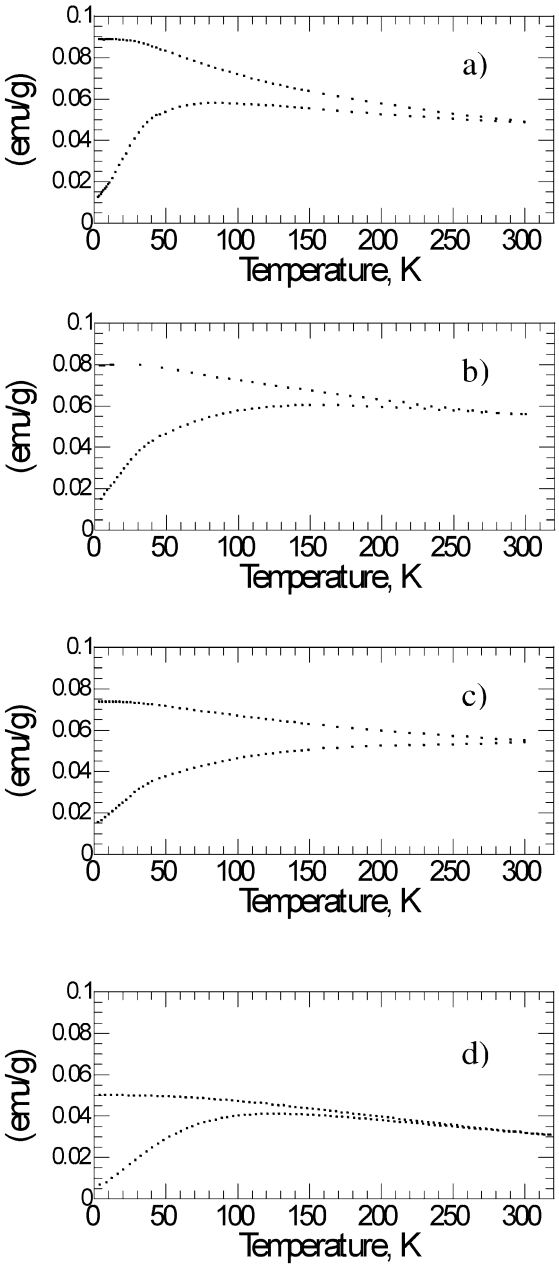

Figure 4. ZFC−FC magnetization of (a) S1050, (b) S1055, (c) S1070, and (d) S0250 samples.

The feature of ZFC and FC susceptibility curves, reported in Figure 4, indicates a superparamagnetic behavior. It should be pointed out that in the samples with $y = 0.1$ (Figure 3a−c) the absence, in the explored temperature range, of a true recombination of the curves indicates that all samples have a fraction of nanoparticles still in the blocked state at room temperature; an approximate value of the unblocking temperature (T_{sep}) around 810 K was estimated by a homemade magnetic balance. This result is surprising if we take into account that bulk alloy samples of the same composition show a rather low anisotropy.[14] It seems therefore reasonable to assume that magnetic moment blocking originates mainly from dipolar magnetic interactions among nanoparticles, as also confirmed by the fact that the three FC curves reach an almost constant value at temperatures lower than 50 K, indicating the possible formation of a collective magnetic state.[15] Because particle interactions are expected to decrease by lowering the alloy amount, mainly as a consequence of increased mean particle distance, the attention was devoted to the sample with the lowest alloy content, S0250, which also shows the lowest value of mean particle size. ZFC and FC curves of this sample are shown in Figure 3d. The ZFC curve shows a more definite maximum, the position of which leads to a value around 120 K for T_{max}, a parameter which is related in a complex way to the average nanoparticle volume and to the presence and strength of particle interactions. The value of T_{sep}, which is 309 K, compared with that obtained for the samples with $y = 0.1$ confirms the hypothesis that blocking in the latter samples is mainly due to particle interactions, taking also into account the lowest value of particle size.

The field dependence of the magnetization recorded at 3 K is shown in Figure 5. None of the samples reaches complete saturation (S1070 being the most distant). The saturation magnetization values (M_s) were obtained by extrapolating the high field regions of the curves.[16]

M_s values, reduced remanent magnetization (M_r/M_s), and coercive field values H_c measured at 3 K are reported in Table 4. At RT the hysteresis loops of samples with $y = 0.1$ show rather low coercivities values which are around 70 Oe. H_c values increase with lowering temperature up to around 400 Oe at 3 K, as expected for a superparamagnetic behavior. The M_s value of each sample at 3 K is lower than that reported for bulk alloys of the same composition.[17,18] The observed differences can depend on the composition of each single particle. Mössbauer spectroscopy data analysis[19] carried out on the samples with $y = 0.1$ indicates the presence of a relevant fraction of oxidated iron ranging from 33% in S1050 to 20% in S1070 samples. This presence has been evidenced by spatially resolved EELS analysis, which shows that the metal oxide is present in the form of a thin and structurally disordered surface layer slightly different on each examined particle.[20] This presence, which can be ascribed to the passivation

(14) Bol, R. In *Materials Science and Technology: A Comprensive Treatment*; Buschow, K. H. J., Ed.; VCH: Weinheim, 1994; vol 3B, Chapter 14.
(15) Fiorani, D.; Dormann, J. L.; Cherkaoui, R.; Tronc, E.; Lucari, F.; D'Orazio, F.; Spinu, L.; Nouges, N.; Garcia, A.; Testa, A. M. *J. Magn. Magn. Mater.* **1999**, *196*, 143.
(16) Morrish, A. H. *The Physical Properties of Magnetism*; Wiley: New York, 1965.
(17) Jiles, D. C. *Introduction to Magnetism and Magnetic Materials,* 2nd ed.; Chapman & Hall: London, 1998.
(18) Turgut, Z.; Huang, M. Q.; Gallegher, K.; McHenry, M. E.; Majetich, S. A., *J. Appl. Phys*. **1997**, *81*, 4039.
(19) Concas, G.; Congiu, F.; Ennas, G.; Piccaluga, G.; Spano, G. *J. Non-Cryst. Solids* **2003**, *330*, 234.
(20) Falqui, A.; Serin, V.; Calmels, L.; Snoeck, E.; Corrias, A. Ennas, G. *J. Microscopy* **2003**, *210*, 80.

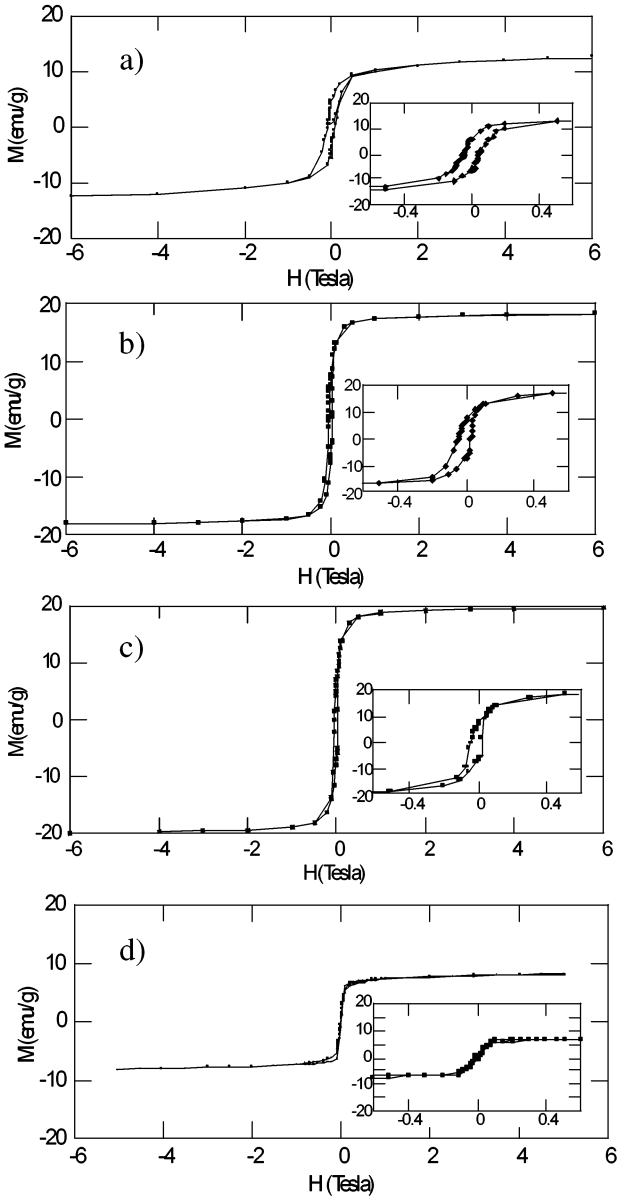

Figure 5. Magnetic hysteresis loop M(H) of (a) S1050, (b) S1055, (c) S1070, and (d) S0250 samples.

process, cannot be revealed by X-ray diffraction and explains the differences in the values of average particle size obtained by TEM. The EELS analysis has also evidenced local differences in alloy composition of nanoparticles. Since magnetic moment of bulk FeCo alloys changes dramatically outside the selected nominal composition range, $x = 0.5-0.7$, the presence in each sample of nanosized particles of non-uniform composition can give a further contribution to the observed M_s behavior.

Table 4. Saturation Magnetization (M_s), Reduced Remanent Magnetization (M_r/M_s), and Coercivity (H_c) Values Measured at 3 K in the Nanocomposite Samples[a]

sample	M_s (emu/g)	M_r/M_s	H_c (Oe)
S1050	16.5(1)	0.36(2)	444(2)
S1055	18.6(1)	0.37(2)	423(2)
S1070	20.1(1)	0.35(2)	402(5)
S0250	9.2(1)	0.08(1)	101(1)

[a] Magnetization data are normalized with respect to the entire mass of the sample.

The reduced remanence values are, for all the samples, lower than 0.5, as expected for randomly oriented, blocked nanoparticles. This result could be ascribed to the occurrence of a nonnegligible fraction of small particles which are still relaxing fast at 3 K or to a small fraction of free paramagnetic iron and cobalt ions.

Conclusions

$(Fe_xCo_{1-x})_y(SiO_2)_{1-y}$ nanocomposites were prepared by reduction in hydrogen flow of silica xerogels containing iron and cobalt. Two sets of samples were prepared: in the first set four y values were selected in the range 0.02−0.20 with $x = 0.50$; in the second set y was kept equal to 0.10 and x was equal to 0.45, 0.50, and 0.70.

The nanocomposites are constituted of spherical crystalline FeCo alloy nanoparticles embedded in an amorphous silica matrix. The mean values of nanoparticle size increase with metal load. All samples show superparamagnetic behavior with unblocking temperature (T_{sep}) well above room temperature for samples with $y = 0.10$, mainly as a consequence of a collective magnetic state due to dipolar magnetic interactions among alloy particles. These interactions decrease with metal load as a consequence of increased particle distances, and T_{max} is around 120 K for the sample with $y = 0.02$. Magnetic properties, in particular M_s values, differ significantly from those of bulk alloy partially due to the presence of a superficial thin layer of iron oxide due to the passivation process and to non-uniform composition of the particles.

Acknowledgment. We acknowledge Ministero dell'Istruzione, dell'Università e della Ricerca (MIUR, PRIN project) and Università di Cagliari. A.F. has been supported by the European Community Improving Human Potential Program under contract HPMH-CT-2000-01007

CM048761E

(21) Stoner, E. C.; Wohlfarth, E. P. *Philos. Trans. R. Soc. London* **1948**, *A240*, 599.